Stokes-darcy fluid flow simulations within 3d Interlock fabrics with capillary effects

Morgan Cataldi, Yanneck Wielhorski, Nicolas Moulin, Augustin Parret-Fréaud, Monica Francesca Pucci, Pierre-Jacques Liotier

ECCM21 – 21st European Conference on Composite Materials
02-05 July 2024, Nantes, France

STOKES-DARCY FLUID FLOW SIMULATIONS WITHIN 3D INTERLOCK FABRICS WITH CAPILLARY EFFECTS

M. Cataldi[1,2], Y. Wielhorski[2], N. Moulin[1], A. Parret-Freaud[3], M. F. Pucci[4] and P-J. Liotier[5]
[1]Mines Saint-Étienne, CNRS, UMR 5307 LGF, 158 Cours Fauriel 42023, Saint-Étienne, France
Email: nicolas.moulin@emse.fr
[2]Safran Aircraft Engines, Rond-point René Ravaud - Réau, 77550 Moissy-Cramayel, France
[3]Safran Tech, Rue des Jeunes Bois, 78772 Magny-les-Hameaux, France
[4]LMGC, IMT Mines Ales, Univ Montpellier, CNRS, Ales, France
[5]Polymers Composites and Hybrids (PCH), IMT Mines Alès, Alès, France

Keywords: 3D interlock fabric, Stokes-Darcy flow, Permeability, Capillarity

Abstract
Resin Transfer Moulding is a widely used process in composite material manufacturing, involving the compaction of a fibrous 3D interlock preform to reach the desired Fibre Volume Fraction (FVF), followed by impregnation with liquid polymer resin. Understanding the dual-scale flows of resin within and between homogeneous equivalent porous yarns is essential for predicting impregnation defects. At the mesoscopic scale, fabric unit cells are characterised by yarn morphology and intra-yarn FVF fields, converted into a permeability tensor field via Darcy's law. This dual-scale nature significantly affects saturated and unsaturated fluid flows, especially due to capillary phenomena within yarns, modelled by a capillary pressure. The aim is to develop a robust numerical framework for simulating fibrous media impregnation at the mesoscopic scale. Fluid flow is modelled by Darcy's equation within porous yarns and by Stokes' equation between yarns, employing a monolithic approach with a mixed velocity-pressure formulation stabilised by a VMS method. Accurate description of resin flow within porous yarns requires locally oriented intra-yarn permeability tensor fields and capillary stress tensor at the resin-air interface. Additionally, pressure enrichment is introduced at the fluid front, represented by a level set function, to capture pressure discontinuity in Darcy domains. Saturated and unsaturated Stokes-Darcy fluid flow simulations are conducted to determine fabric permeability as a function of global FVF at different compactions and to evaluate the influence of capillary phenomena on the impregnation scenario.

1. Introduction

3D interlock fabrics, filled with a thermoset resin through RTM (Resin Transfer Moulding) processes, yield high-performance composite materials with tailored mechanical properties. Due to their light weight compared to their mechanical properties, they are well suited for aeronautics applications. To ensure desired mechanical properties, a precise monitoring of manufacturing processes is essential. Fabric permeability emerges as a key parameter of the process, and thus needs to be precisely characterised through either fluid flow experiments or numerical simulations [1]. However, such a value comes along with its associated variability resulting from many factors. Among them, the variability of the intra-yarn permeability is of particular interest, since the weaved yarns are also porous materials which permeability is linked to its fibres local microstructure. Since the fluid flows both within and around the porous yarns, this dual-scale nature has to be taken into account within models. In addition, dry spots may appear at the end of the impregnation and hinder the mechanical properties of the composite parts manufactured. They are the result of both the process parameters and material properties of the fabric and porous yarns within it.

Our numerical simulations are performed on 3D woven models that are generated using techniques found in literature [2]. Many studies, both on idealized woven patterns [3] or X-ray micro-tomographies [4], analyse the variations of the fabric effective permeability. In these studies, the intra-yarn permeability tensor is generally set to change homogeneously over the yarns between different simulations [5]. However, due to local deformations of the yarns during the fabric forming process, the intra-yarn FVF varies along the yarns. The 3D woven model generation used in this work takes into account this phenomenon to compute an intra-yarn FVF field, which is then used to get an intra-yarn permeability field. The effect of its variability, induced by the fabric forming process, on the overall fabric permeability can then be studied.

Several methods exist to model the dual-scale flow problem both around and within the homogeneous equivalent porous yarns [6]. But to deals with domains with high properties contrast, such as in 3D interlocks, the Stokes-Darcy coupled problem is used in our simulations to model the double-scale fluid flow. It is solved by a mixed velocity-pressure Finite Element (FE) formulation with a monolithic approach detailed in previous works [7,8], and stabilised by a Variational MultiScale Method (VMS) method.

In transient simulations, the fluid front is modelled by a levelset function [9]. It is well suited for modelling its complex tropological changes during dual-scale flows. The levelset method allows to sharply describe the fluid front where capillary forces normal to the interface are prescribed. A capillary stress tensor is used in our simulations and its component scalar values can come from experiments [10,11] or numerical simulations at the microscopic scale [12].

2. Materials and Methods

2.1. Digital materials

The material used is a 3D angle-interlock woven fabric simulated with Multifil software [10]. The unit cell (18.9×18.9×4.9 mm^3) is composed of 27 yarns. This 3D fabric is computed with the woven pattern and the yarn features (the number of carbon fibres per yarn, their mechanical properties and their twist). The yarn deformations are then computed by taking into account an enriched kinematics beam model and contact-friction interactions. The resulting non-periodic unit cell is described by the meso-scale yarn morphology and the intra-yarn FVF. This last characteristic shown in Figure 1 is an upscaling of the microscopic intra-yarn morphology. Yarns are considered as homogeneous equivalent media characterised geometrically by consecutive sections attached to a neutral fibre, and by a permeability tensor. Both “as-woven” (not yet compacted) and “compacted” (as-manufactured) unit cells, along with their intra-yarn FVF field are shown in Figure 1.

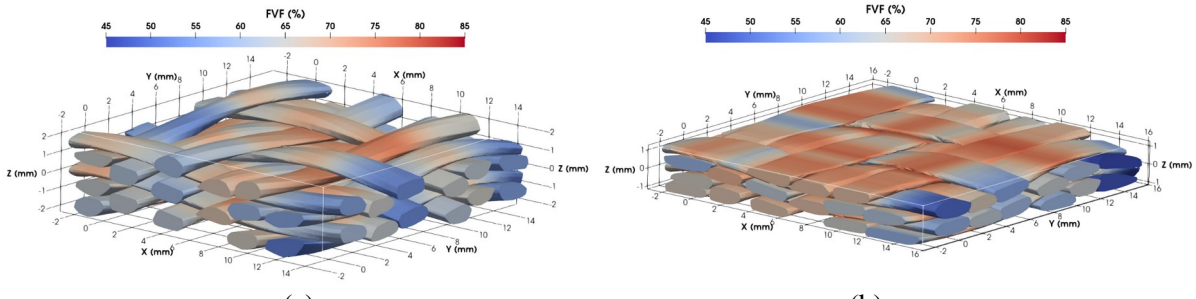

(a) (b)

Figure 1. (a) as-woven and (b) compacted 3D interlock unit cells with their intra-yarn FVF field, respectively 29% and 58% global FVF [14].

2.2. Intra-yarn permeability

The intra-yarn permeability tensor is assumed to be transversely isotropic in its principal coordinate system $(\mathbf{e}_I, \mathbf{e}_{II}, \mathbf{e}_{III})$ attached to a neutral fibre [14]. According to Gebart's law in hexagonal arrangement [15], the eigenvalues can be computed using equations (Eq. 1), where $R = 2.6$ µm is the fibre radius, V_f is the intra-yarn FVF value, K_L is the longitudinal permeability and K_T is the transverse one.

$$\begin{cases} K_L &= R^2 \left[\dfrac{8}{53} \dfrac{(1-V_f)^3}{V_f^2} \right] \\ K_T &= R^2 \left[\dfrac{16}{9\pi\sqrt{6}} \left(\sqrt{\dfrac{\pi}{2\sqrt{3}V_f}} - 1 \right)^{\frac{5}{2}} \right] \end{cases} \tag{1}$$

The resulting intra-yarn permeability values with their Probability Density Functions (PDF), means μ and standard deviations σ for both as-woven and compacted unit cells are shown in Figure 2.

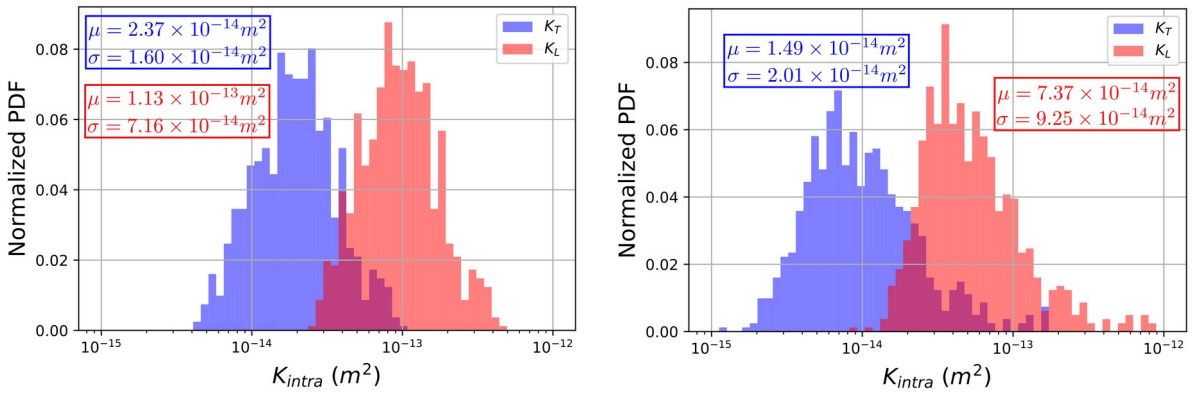

(a) (b)

Figure 2. Probability Density Functions (PDF) of intra-yarn permeabilities for (a) as-woven and (b) compacted unit cells [14].

2.3. Numerical strategy for saturated flows

The aim of this study is to perform simulations of the saturated double-scale fluid flow within both as-woven and compacted unit cells in order to compute their effective permeability tensor, a.k.a. the saturated permeability. The steady-state flow is assumed to be incompressible and laminar (small Reynolds numbers $Re \ll 1$). The fluid behaviour is considered to be Newtonian with a dynamic viscosity $\mu = 0.2$ Pa.s. The physical model summarised in Figure 3 couples Stokes' equations in the domain around the yarns and Darcy's equations within them, where $\mathbf{K}_{intra}$ is the intra-yarn permeability tensor.

Both yarns and spaces between them are meshed with tetrahedra forming an unstructured grid. This kind of mesh was chosen instead of a structured grid because it allows to mesh more efficiently complex geometries such as those involved in this work, and it is required by the FE formulation. The unit cell is firstly meshed with voxels and then remeshed with tetrahedra [14]. Moreover, the mesh is conformal, meaning that nodes belonging to elements from both parts of the interface Γ (Stokes-Darcy interface in Figure 3) are matching on the interface itself. This feature allows an explicit description of the different regions within the unit cell. The characteristic voxel size ranges from 70 to 100 µm, and the resulting tetrahedral meshes have between 1 and 8 million nodes.

The Stokes-Darcy coupled problem illustrated in Figure 3 is solved by the Z-set software [16] using a monolithic approach and a mixed velocity-pressure Finite Element (FE) formulation. Piecewise linear

approximations are considered for both velocity and pressure fields. Such a P1/P1 formulation is not stable, so a Variational MultiScale (VMS) method is introduced to stabilize it. This formulation has been widely presented in former articles [7,8], highlighting in particular the weak formulation of the stabilised Stokes-Darcy coupled problem.

One simulation per direction needs to be performed to compute the effective permeability tensor of the unit cell. A pressure drop ΔP is applied respectively in the X, Y and Z directions, while for the other unit cell boundaries a null normal velocity condition is given, as shown in Figure 3. Note that no periodic boundary condition can be applied on this unit cell since it is not periodic.

The effective permeability $\mathbf{K}_{eff}$ of the unit cell is post-processed through the 3D-generalized Darcy law. All the flow rate values involved are computed by integrating the velocity field component normal to the unit cell boundary. All the pressure values involved are computed as the mean value of the pressure over the corresponding unit cell boundary.

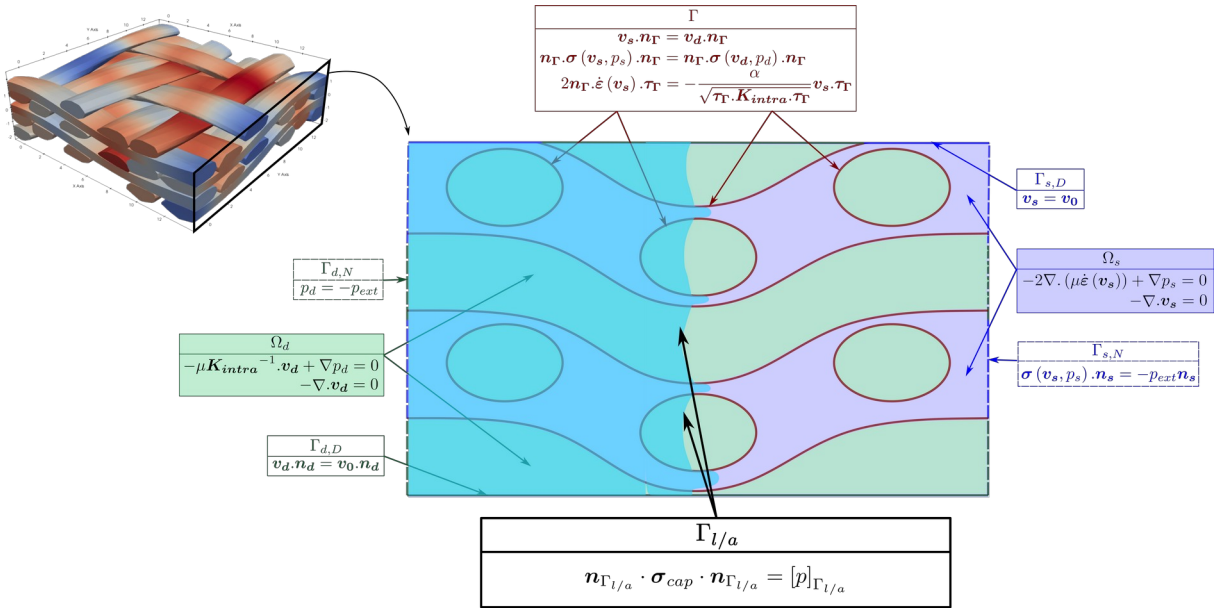

Figure 3. Physical model of the Stokes-Darcy coupled problem (simplified cross-section diagram).

2.4. Numerical strategy for transient flows

The aim is to perform simulations of the transient dual-scale fluid flow within both as-woven and compacted unit cells, where resin progressively replaces air within the preform during the filling process. In addition to the Stokes-Darcy coupling and the numerical strategy to solve it, previously described, the resin-air interface needs to be modelled and captured through time. The level-set method describes the interface through a levelset field $\phi(\mathbf{x}, t)$ corresponding to the distance between a given point $\mathbf{x}$ and the interface. To model the motion of the interface, the field is then transported through an advection equation. This requires an advective velocity that corresponds to the fluid velocity $\mathbf{v}$:

$$\frac{\partial \phi}{\partial t} + \mathbf{v} \cdot \nabla \phi = 0 \tag{2}$$

This problem corresponds to a hyperbolic first-order partial derivative equation. Initial and boundary conditions are thus added so that the problem can be solved in the computation domain. A time-implicit discretisation is achieved with a Crank-Nicolson scheme and a Streamline Upwind Petrov-Galerkin (SUPG) stabilizes the FE formulation. Because the field ϕ is a signed distance to the interface, this property needs to be ensured through the simulation via a reinitialisation step following the convection step. Taking into account this moving flow front into Stokes-Darcy equations (Figure 3) consists of simply replacing the constant resin viscosity μ by the liquid viscosity $\mu_l = 0.2$ Pa.s in

the filled domain (when $\phi > 0$) and equal to $\mu_a = 1.10^{-3}$ Pa.s in the empty domain (when $\phi < 0$). The air is assumed to be a Newtonian incompressible fluid having a very low viscosity $\mu_a \ll \mu_f$.

Capillary effects occurring at the microscopic scale between the yarn fibres are to be upscaled at the mesoscopic scale within the homogeneous equivalent porous yarns. A transverse isotropic capillary stress tensor $\boldsymbol{\sigma}_{cap}$ is thus introduced within the Darcy zones (Figure 3) to account for the pressure discontinuity at the liquid/air interface $\Gamma_{l/a}$ of normal $\mathbf{n}$ such as [17]:

$$\mathbf{n} \cdot \boldsymbol{\sigma}_{cap} \cdot \mathbf{n} = [p]_{\Gamma_{l/a}} \tag{3}$$

The capillary stress and jump of viscosities across $\Gamma_{l/a}$ generate discontinuities for both the pressure and the pressure gradient within mesh elements crossed by $\Gamma_{l/a}$ (Figure 3). It is addressed by enriching the pressure field with new degrees of freedom which are then condensed, as detailed in [17].

3. Results and perspectives

Analysis of the streamlines in the simulations of the double-scale saturated flow in Figure 4 suggests that the majority of the fluid flows around the yarns, which is highlighted by the greater velocity magnitude in these areas. The low intra-yarn permeability values, in the range $[10^{-14}; 10^{-12}]$ m² compared to the inter-yarn channels width explains why the fluid does not flow well through the yarns. As a result, variations of the effective permeability tensor $\mathbf{K}_{eff}$ were induced by variations of the intra- yarn FVF field in a very limited way.

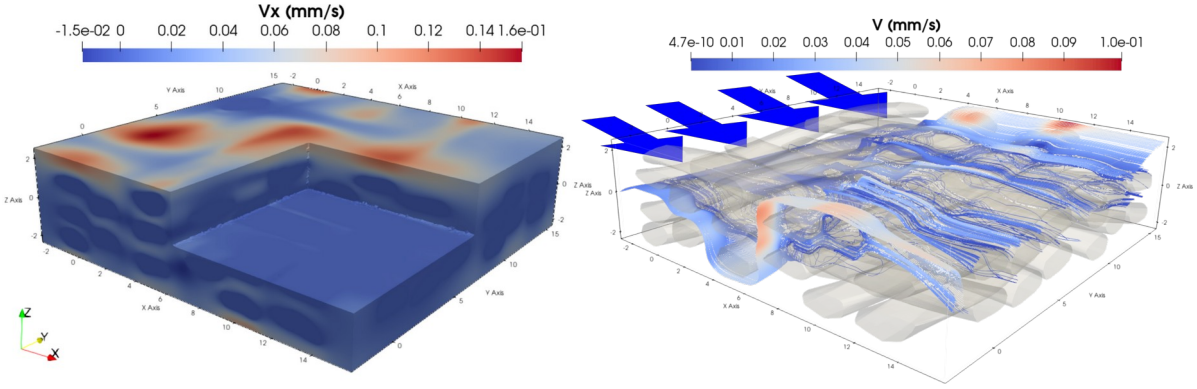

(a) (b)

Figure 4. (a) Velocity field and (b) streamlines from the inlet boundary in the as-woven unit cell.

On the contrary, changes in the mesoscopic unit cell morphology are of first importance when studying its permeability tensor $\mathbf{K}_{eff}$. This is highlighted in Table 1, where the fabric compaction leads to a reduction of about 2 orders of magnitudes for its diagonal components K_{xx}, K_{yy} and K_{zz}. This is due to the huge reduction of inter-yarn spaces trough the compaction, thus increasing the unit cell global FVF value (with porous yarns) from 29% to 58%.

Table 1. Effective permeabilities of the as-woven (29% FVF) and compacted (58% FVF) unit cells.

FVF [%]	K_{xx} [m²]	K_{yy} [m²]	K_{zz} [m²]
29	6.10^{-8}	9.10^{-8}	2.10^{-8}
58	5.10^{-10}	2.10^{-9}	2.10^{-9}

Moreover, the velocity field shown in Figure 4 highlights preferential edge flows characterized by high velocity magnitudes. This implies that, in addition to flowing around the yarns, the fluid mainly flows near the unit cell boundaries. Consequently, the effective permeability tensor $\mathbf{K}_{eff}$ of the unit

cell is overestimated. To take it into account, a geometrical reduction of its boundaries is performed, as illustrated in Figure 5, prior to the numerical simulation in order to ensure that the fluid flows within the weaving pattern. This reduction of 10% eliminates most of the preferential edge flows and thus allows for a more accurate computation of the permeability tensor, as shown in Table 2.

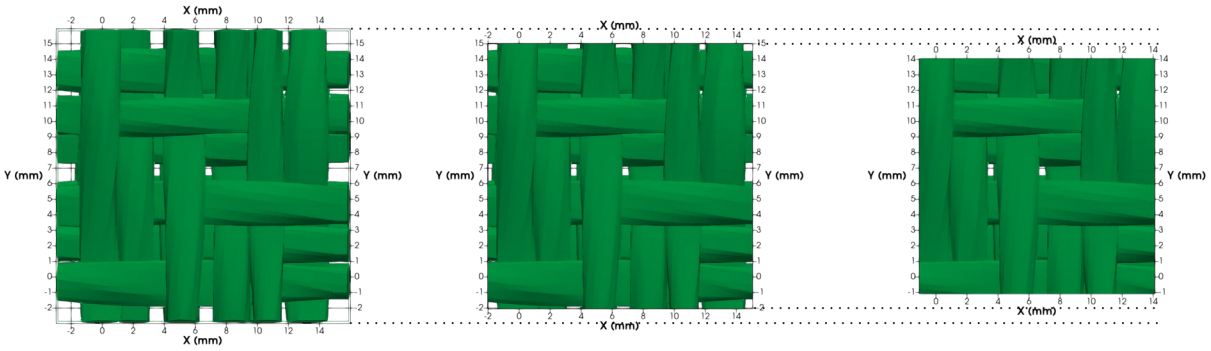

Figure 5. Top view of an as-woven unit cell reduced by 0%, 10% and 20% on the (X, Y) plane.

Table 2. Effective permeabilities of of the whole and reduced as-woven unit cell.

UC reduction [%]	K_{xx} [m²]	K_{yy} [m²]	K_{zz} [m²]
0	6.10^{-8}	9.10^{-8}	2.10^{-8}
10	4.10^{-8}	6.10^{-8}	3.10^{-9}
20	4.10^{-8}	5.10^{-8}	2.10^{-9}

A numerical simulation of the transient flow in the X direction was carried out on the woven unit cell. The filling of the as-woven unit cell can be seen in figure 6 at two different stages. As in the saturated regime, the fluid flows preferentially around the yarns. However, due to the capillary pressure acting within the yarns, the latter become impregnated. Transient flow simulations will allow to study the location of dry areas and impregnation defects within the fabric unit cells, and in particular on the effect of capillary pressure determined from experiments and the level of compaction. A particular interest will be given to both physical and numerical aspects occurring near the flow front and the yarn-channel numerical interface.

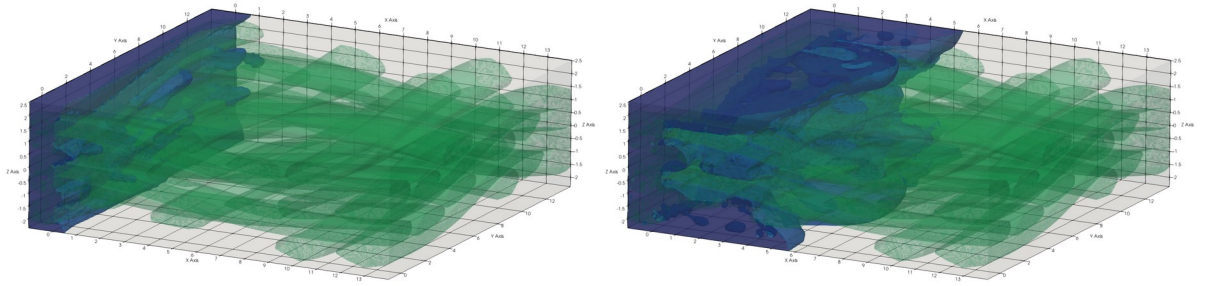

(a) (b)

Figure 6. Filling simulation of the as-woven unit cell; (a) beginning and (b) middle of the simulation.

Acknowledgments
Authors acknowledge the support of a PhD grant N°2021/0156 from ANRT and Safran Aircraft Engines.

References
[1] M.A. Ali, R. Umer, K. Khan, S. Bickerton, W.J. Cantwell. Non-destructive evaluation of through-thickness permeability in 3D woven fabrics for composite fan blade applications. Aerosp. Sci. Technol., (2018) 82:520-533.
[2] Y. Wielhorski, A. Mendoza, M. Rubino, S. Roux. Numerical modeling of 3d woven composite reinforcements: A review, Compos. - A: Appl. Sci. Manuf., (2022) 154:106729.
[3] Q Wang, B Mazé, HV Tafreshi, B Pourdeyhimi. A note on permeability simulation of multifilament woven fabrics. Chem. Eng. Sci., (2006) 61(24):8085-8088.
[4] MA Ali, R Umer, KA Khan, WJ Cantwell. XCT-scan assisted flow path analysis and permeability prediction of a 3D woven fabric. Compos. - Part B: Eng., (2019) 176:107320.
[5] A. Geoffre, Y. Wielhorski, N. Moulin, J. Bruchon, S. Drapier, P.-J. Liotier. Influence of intra-yarn flows on whole 3D woven fabric numerical permeability: from Stokes to Stokes-Darcy simulations, Int. J. Multiph. Flow, (2020) 129:103349.
[6] E. Syerko, C. Binetruy, S. Comas-Cardona, A. Leygue. A numerical approach to design dual-scale porosity composite reinforcements with enhanced permeability. Mater. Des., (2017) 131:307-322.
[7] L Abouorm, M Blais, N Moulin, J Bruchon, S Drapier. A Robust Monolithic Approach for Resin Infusion Based Process Modelling, Key Eng. Mater., (2014) 611:306-315.
[8] M. Blais, N. Moulin, P.-J. Liotier, S. Drapier. Resin infusion-based processes simulation: Coupled Stokes-Darcy flows in orthotropic preforms undergoing finite strain. Int. J. Mater. Form., (2015) 10:43-54.
[9] S. Osher, R.P. Fedkiw. Level set methods: an overview and some recent results, J. Comput. Phys, (2001) 169(2):463-502.
[10] H. Teixidó, G. Broggi, B. Caglar, V. Michaud. Measurement and modelling of dynamic fluid saturation in carbon reinforcements, Compos. - A: Appl. Sci. Manuf., (2023) 169:107520.
[11] M.F. Pucci, P.-J. Liotier, S. Drapier. Capillary wicking in a fibrous reinforcement - Orthotropic issues to determine the capillary pressure components, Compos. - A: Appl. Sci. Manuf., (2015) 77:133-141.
[12] A. Geoffre, N. Moulin, J. Bruchon, S. Drapier. Reappraisal of Upscaling Descriptors for Transient Two-Phase Flows in Fibrous Media. Transp. Porous Med., (2023) 147:345-374.
[13] D. Durville, I Baydoun, H Moustacas, G Périé, Y Wielhorski. Determining the initial configuration and characterizing the mechanical properties of 3D angle-interlock fabrics using finite element simulation, Int. J. Solids Struct., (2018) 154:97-103.
[14] M. Cataldi, Y. Wielhorski, N. Moulin, M.F. Pucci, P.-J. Liotier. Accounting for mesoscale geometry and intra-yarn fiber volume fraction distribution on 3D angle-interlock fabric permeability, Int. J. Multiph. Flow, (2024) 173:104721.
[15] B.R. Gebart. Permeability of Unidirectional Reinforcements for RTM. J. Compos. Mater., (1992) 26(8):1100-1133.
[16] Z-set software. http://www.zset-software.com.
[17] K. Andriamananjara, N. Moulin, J. Bruchon, P.-J. Liotier, S. Drapier. Numerical modeling of local capillary effects in porous media as a pressure discontinuity acting on the interface of a transient bi-fluid flow, Int. J. Mater. Form., (2019) 12(4):675-691.
[18] M.F. Pucci, P.-J. Liotier, S. Drapier. Capillary wicking in a fibrous reinforcement - orthotropic issues to determine the capillary pressure components. Comp. Part A, (2015) 77:133-141.